ISSN 1 746-7233, England, UK
World Journal of Modelling and Simulation
Vol. 11 (2015) No. 1, pp. 33-42

Numerical simulation of gas flow through a biofilter in lung tissues

Anju Saini*, V. K. Katiyar, Pratibha

Department of Mathematics, Indian Institute of Technology Roorkee, Roorkee 247667, India

(*Received November 2 2014, Accepted December 12 2014*)

Abstract. Nanoparticles are potentially hazardous to human health; thus, it is necessary to control their motion in air. We need a biofilter to protect from nanoparticles which enter human lung and damage it. Biofiltration refers to the biological transformation or treatment of contaminants present in the gas phase, usually air. Biofilter is typically a porous media. Supported on the ideal biofilter model, numerical simulation is carried out to examine the effect of Darcy number and porosity on removal efficiency of low headloss biofilter. The generalized Navier-Stokes equations are applied making various hypotheses. It is found that the Darcy number has determinant influence on the removal efficiency, and the effect of porosity on removal efficiency is very weak at lower Darcy numbers but very strong at higher Darcy numbers. The aim of this paper is to study the effect of Darcy number and porosity on air removal efficiency of biofilter.

Keywords: lung tissue, darcy number, biofilter, porous flow, removal efficiency

1 Introduction

Toxicity of nanoparticles is of rising concern due to fast development and growth of nanotechnology[6, 18]. Up till now, interactions of nanoparticles with the human body are not totally understood, while an epidemiological study explained that surplus morbidity from fine particles resulted from air pollution affairs in several U.S. cities[12]. When nanoparticles are engaged or ingested, their performance diverges from larger particles. They create a particularly huge health risk because they are expected to be more reactive and toxic than larger particles. Depending on the field of application, nanoparticles may enter the body via inhalation, dermal, oral or injection exposure routes. Carbon nanotubes have aspect ratios comparable to asbestos fibers. If inhaled then the nanotubes may probably quite easily move through the airways down to the alveoli, where they may get stuck and initiate different diseases like asthma, COPD etc. Biofiltration is an emerging technology used in pollution control. It can be used for both water and air purification, with a wide range of contaminants. Biofiltration uses biological means for the degradation of pollutants in either an air or water stream. It has been applied to remediate air contaminated with volatile organic compounds (VOCs) and other gases[1, 16, 21, 27]. This technology is preferred as a pollutant removal technique due to its low investment and operating cost, high removal efficiency, reliable operating stability and low amount of secondary pollution[25].

Biofilters are usually porous media. A porous medium is a material containing pores (voids). The pores are typically filled with a fluid (liquid or gas)[22]. Usually, fluids flow through biofilter media can be precisely calculated by the established models, such as the Darcy model[5]. Darcy's law allows the analysis of laminar fluid flow through porous media. Generally, Darcy's law holds for (1) saturated and unsaturated flow, (2) steady-state and transient flow, (3) flow in homogeneous and heterogeneous systems, (4) flow in isotropic and anisotropic media, and (5) flow in both rocks and granular media. The lower limit for the validity of Darcy's law is a threshold gradient that may be required to start flow. Darcy's law and the modified-Ergun equation were effectively used to model gas flow through various mixtures. The media must also have a high porosity for minimizing pressure drop across the biofilter, good moisture holding capacity, and a sufficiently

* Corresponding author. *E-mail address*: anju.iitr@gmail.com

long useful life[14]. Mayerhofer et al.[17] investigated the pressure drop over a packed bed of irregularly shaped wood particles by determining the coefficients in the drag force term through well-designed experiments.

The biofilters are operated continuously. The concentrations of the compounds and nitrogen dioxide in the inlet and the outlet streams (gas and liquid) are measured for each biofilter. The effect of dust described by two parameters, the concentration and relaxation time, which measure the rate at which the velocity of a dust particle adjusts to change the air velocity and depends upon the size of individual particles. The alveolar sacs can be considered as a biofilter that removes particles from the inspired air.

The purpose is to study the effect of Darcy number and porosity on the velocities of fluid and dust particles and air removal efficiency to get a better performance of biofilter.

2 Mathematical model

In a circular tube (like capillaries of alveolar sacs), we have considered the region on the axis of the tube and the x-axis along the axis of the tube. The motion of the dusty viscous, incompressible air is considered along the axis of the tube under the influence of the time dependent pressure gradient. The boundary conditions for the fluid are same as those for classical fluid and no particle boundary conditions are required. The air velocity is set to be zero on the walls.

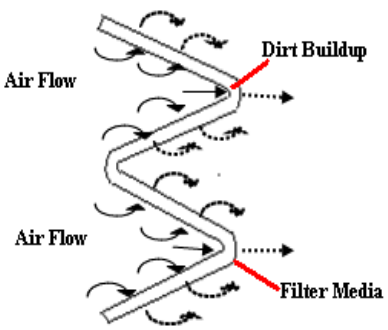

Fig. 1. Principles of filtration

2.1 Governing equations

There are a number of models existing for porous flow. At the present work we have used the representative elementary volume (REV) scale model recommended by Nithiarasu and Ravindran[19]. The appropriate momentum equations in cylindrical polar coordinates are

$$\frac{\partial u}{\partial t} + \frac{u}{\varepsilon}\frac{\partial u}{\partial r} = -\frac{\varepsilon}{\rho}\frac{\partial p}{\partial r} + \nu\left(\frac{\partial^2 u}{\partial r^2} + \frac{1}{r}\frac{\partial u}{\partial r}\right) + F, \tag{1}$$

$$m\frac{\partial v}{\partial t} = k(u - v), \tag{2}$$

where u and v are the velocity of air flow and dust particles respectively, ρ is the air density, ε is the porosity, ν is the kinematic viscosity parameter, p is the fluid pressure, m is the mass concentration of dust particles, k is the Stokes resistance coefficient which, for spherical particles, is 6rp, being the coefficient of viscosity of the air and r_p the radius of the particles. F stands for the entire body force because of the existence of porous media and additional external force fields, and is formulated as

$$F = -\frac{\varepsilon\nu}{K}u + \frac{kN_0}{\rho}(v - u), \tag{3}$$

where v is the kinematic viscosity of air, N_0 is the number density of the dust particles. The permeability K depends on the porosity ε based on the Ergun's empirical formula[8] and can be formulated as [24].

$$K = \frac{\varepsilon^3 d_p^2}{150(1-\varepsilon)^2}, \tag{4}$$

where d_p is the diameter of the solid particles.

2.2 Initial conditions

All The initial conditions are at $t \leq 0$,

$$u = v = \frac{\partial u}{\partial t} = 0. \tag{5}$$

3 Methodology

3.1 Transformation of the governing equations

Introducing the following non-dimensional quantities

$$r^* = \frac{r}{a},\ \ p^* = \frac{pa^2}{\rho\nu^2},\ \ t^* = \frac{t\nu}{a^2},\ \ u^* = \frac{ua}{\nu},\ \ v^* = \frac{va}{\nu}$$

in the Eqs. (1) and (2) (dropping the stars) we get

$$\frac{\partial u}{\partial t} + \frac{u}{\varepsilon}\frac{\partial u}{\partial r} = -\varepsilon\frac{\partial p}{\partial r} + \left(\frac{\partial^2 u}{\partial r^2} + \frac{1}{r}\frac{\partial u}{\partial r}\right) + B(v-u) - \frac{\varepsilon}{Da}u, \tag{6}$$

$$\frac{\partial v}{\partial t} = \frac{u-v}{\tau}. \tag{7}$$

where

$$B = \frac{M}{\tau} = \frac{N_0 k a^2}{\mu},\ \ M = \frac{N_0 m}{\rho},\ \ \tau = \frac{\nu m}{ka^2},\ \ Da = \frac{K}{a^2}.$$

The pressure gradient may be assumed in the form

$$-\frac{\partial p}{\partial r} = P_0 e^{-\lambda t}. \tag{8}$$

The finite difference scheme is used to solve the governing transformed equation by using central difference approximations for all the spatial derivatives[23]. The iterative method has been found to be quite effective in solving the equation numerically for different time periods. The result appeared to converge with accuracy of the order 10^{-5} when the time step was chosen to be $\Delta t = 0.00001$ and $\Delta r = 0.01$ along the axial directions. These results are subsequently used to solve equations numerically.

4 Discretization of the components

The discretization of velocity $u(r,t)$ is written as $u(r_i, t_i)$ or $u_{i,i}$. We define

$$r_i = i.\Delta r;\ \ i = 0, 1, 2 \cdots N \ \text{ where } \ r_N = 1.0,$$
$$t_j = j.\Delta t;\ \ j = 0, 1, 2, \cdots M.$$

For using discretization in the Eq. (6), at $r = 0$,

$$\lim_{r\to 0}\frac{1}{r}\frac{\partial u}{\partial r}=\lim_{r\to 0}\frac{\partial^2 u}{\partial r^2}. \tag{9}$$

The Eq. (6) becomes

$$\frac{\partial u}{\partial t}+\frac{u}{\varepsilon}\frac{\partial u}{\partial r}=-\varepsilon\frac{\partial p}{\partial r}+2\frac{\partial^2 u}{\partial r^2}+B(v-u)-\frac{\varepsilon}{Da}u. \tag{10}$$

The velocity of fluid can be calculated from the Eq. (10) (at $r=0$) and its discretized form is

$$\begin{aligned}u_{i,j+1}=&\left(1-B.\Delta t-C.\Delta t-\frac{4.\Delta t}{\Delta r^2}\right)u_{i,j}+\Delta t.\left(\frac{2}{\Delta r^2}-\frac{u_{i,j}}{2.\varepsilon.\Delta r}\right)u_{i+1,j}\\&+\Delta t.\left(\frac{2}{\Delta r^2}+\frac{u_{i,j}}{2.\varepsilon.\Delta r}\right)u_{i-1,j}+B.\Delta t.v_{i,j}+P_0.\varepsilon.\Delta t.e^{-\lambda t}\end{aligned} \tag{11}$$

Also from the Eq. (6) at $0<r\leq 1$,

$$\begin{aligned}u_{i,j+1}=&\left(1-B.\Delta t-C.\Delta t-\frac{2.\Delta t}{\Delta r^2}\right)u_{i,j}+\Delta t.\left(\frac{1}{\Delta r^2}-\frac{u_{i,j}}{2.\varepsilon.\Delta r}+\frac{1}{2.r.\Delta r}\right)u_{i+1,j}\\&+\Delta t.\left(\frac{1}{\Delta r^2}+\frac{u_{i,j}}{2.\varepsilon.\Delta r}-\frac{1}{2.r.\Delta r}\right)u_{i-1,j}+B.\Delta t.v_{i,j}+P_0.\varepsilon.\Delta t.e^{-\lambda t}\end{aligned} \tag{12}$$

The velocity of dust particles can be calculated from the Eq. (7) and its discretized form is

$$v_{i,j+1}=\left(1-\frac{\Delta t}{\tau}\right)v_{i,j}+\frac{\Delta t}{\tau}u_{i,j}. \tag{13}$$

The initial and boundary conditions in discretized form are as follows:

$$u_{i,1}=v_{i,1}=0,\ \ u_{2,j}=u_{0,j},\ \ u_{N+1,j}=0. \tag{14}$$

Now, we solve the problem using above discretization techniques for velocity.

5 Results and discussion

Numerical computations have been carried out using the following parameter values[2, 9, 11]. $P_0=101.325kPa$, $m=0.0002kg/l$, $d_p=100nm$, $\rho=1.185kg/m^3$, $v=1.5210-5m^2/s$, $N_0=0.025041012/m^3$, $a=0.5\mu m$, $\varepsilon=0.6$.

Velocities of air and dust particles on the wall have been represented graphically with variable axial positions, time, porosity and Darcy number. Dullien[7] declared that flow through packed beds can be examined by two approaches. The first is to describe the flow inside conduits and the second is to describe flow around solid objects absorbed in the fluid. For low and intermediate porosities, the conduit flow approach is more suitable. For very high porosities, the flow around submerged objects approach is more appropriate. So, we have considered the value of porosity above 50% of total value.

5.1 Porosity effect on biofilter

Void ratio is the proportion of free space volume in a biofilter to the total biofilter volume. In a biofilter there are voids that are not filled in by the media. High void ratios reduce clogging and allow for air to move more freely in the biofilter. Remember, biofilters work by allowing a thin film of water to flow across media surfaces. Biofilters with low void ratios tend to interrupt this thin flow of water and trap many solid particles. Clogged biofilters must be cleaned, which often leads to reduced biofilter efficiency.

From Fig. 2 it is clear that at porosity $\varepsilon=0.6$, the velocity of the air increases with time. It has attained maximum velocity at the center of the tube at $r=0$ and occupied maximum value earlier at $t=0.1$. After that, the velocity of air decreases simultaneously as time increases and became zero on the tube wall. Due to

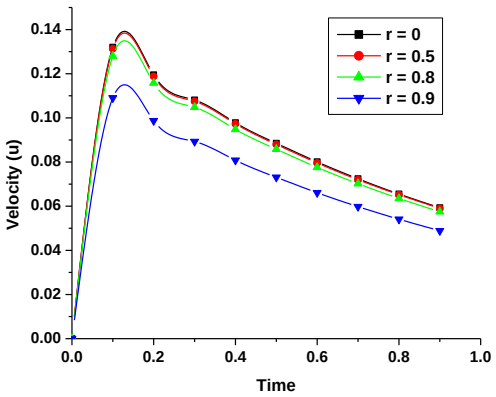

Fig. 2. Velocity profile for the air flow with time for different radial positions at porosity 0.6

classical flow, initially the effects of particles are almost negligible therefore the highest velocity is attained. Later the particle hinders the flow and the subsequent velocity reduces.

In Fig. 3 at porosity $\varepsilon = 0.9$, the velocity of the air increases gradually with time. It attains maximum velocity at $t = 0.2$ at the center of the tube and after that decreases simultaneously as time increases. The velocity depends on the porosity. From Fig. 2 and 3 it is clear that at porosity $\varepsilon = 0.9$, the velocity profiles for the air flow are greater than that at porosity $\varepsilon = 0.6$.

Fig. 4 and 5 show the velocity profiles for the dust particles near the initial point of the tube with the time at porosity 0.6 and 0.9 respectively. Velocities of the dust particles increase with decreasing values of radial distance and increasing values of time. From the figures we examine that the radial parameter works gradually to explain its effect, i.e. velocity of the dust particles increases regularly with time. From Fig. 4 and 5 it is clear that at porosity $\varepsilon = 0.9$, the velocity profiles for the dust particles increase more than that at porosity $\varepsilon = 0.6$.

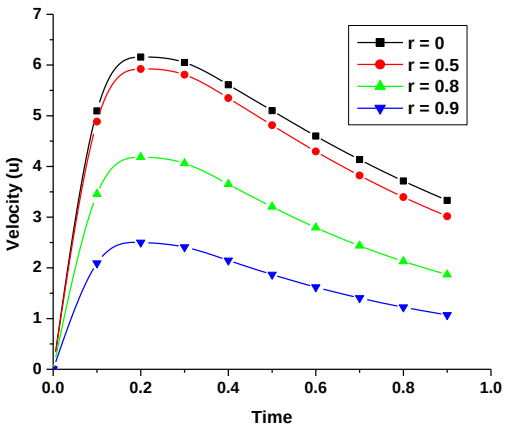

Fig. 3. Velocity profile for the air flow with time for different radial positions at porosity 0.9

5.2 Darcy number effect on biofilter

Fig. 6 and 7 are shown the variations of velocity for the fluid for different values of r with time. As r increases, the velocity decreases for the fluid. Velocity of the fluid at Darcy number 10^{-1} is greater than at Darcy number 10^{-2} for fixed axial position. From Fig. 6 and 7, it is clear that the velocity of the air increases

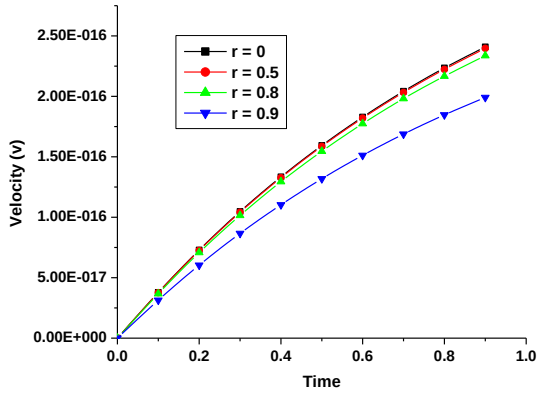

Fig. 4. Velocity profile for the particle with time for different radial positions at porosity 0.6

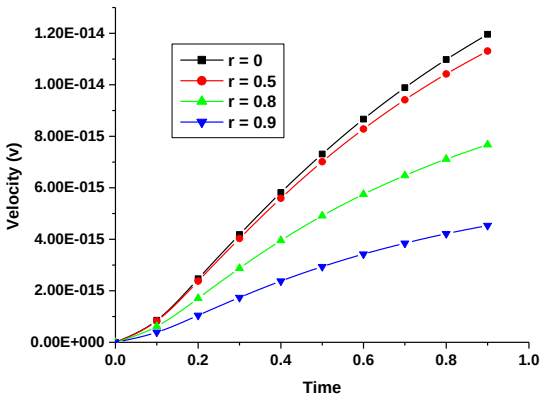

Fig. 5. Velocity profile for the particle with time for different radial positions at porosity 0.9

gradually as time increases. After some time it attains maximum velocity at $t = 0.3$ (Fig. 6) and it attains maximum velocity earlier at $t = 0.15$ (Fig. 7) after that it decreases simultaneously as time increases. This result of Darcy number presents good agreement with porosity ε.

Effects of Darcy number Da on velocity of the dust particles close to the starting point of the tube are given away in Fig. 8 and 9. From Fig. 8 and 9, it is obvious that velocity of the dust particles increase with time. It is shown that the particles attains maximum velocity on the center of tube $r = 0$. It is also clear that at Darcy number 10^{-2}, the particle velocity increases more gradually with time than at Darcy number 10^{-1}.

Further, from Fig. 2-9 we conclude that at a particular time position, the air velocity is greater than the particle velocity. Near the boundary, the dust particles exhibit a sudden change in velocity and this tendency decreases with the porosity and the Darcy number.

5.3 Time of travel model

The traveling time of air is an essential parameter to estimate the efficiency in the biofilter. If the traveling time is very short, the biofilter cannot remove the air pollutants successfully; if the traveling time is very lengthy, the efficiency of the biofilter would be very little. To compute the traveling time of air in biofilter, the inlet height is separated uniformly into N nodes and then the path lines passing through these N nodes are traced to find out the traveling time of every one air particle. The Darcy number is determinant factor for traveling time[26]. At the similar porosity $\varepsilon = 0.6$, the traveling time raises above 100 times when the Darcy number is reduced from 10^{-1} to 10^{-3}.

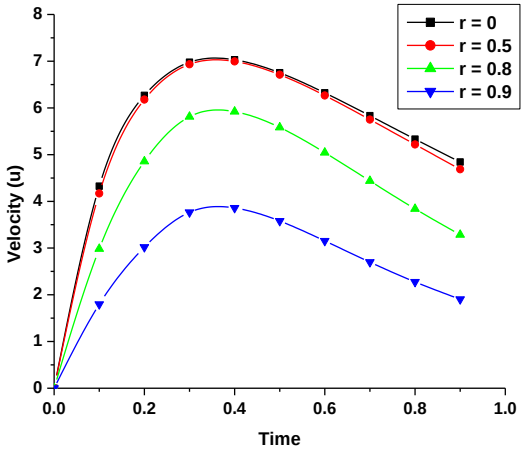

Fig. 6. Velocity profile for the air flow with time for different radial positions at Darcy number 10^{-1}

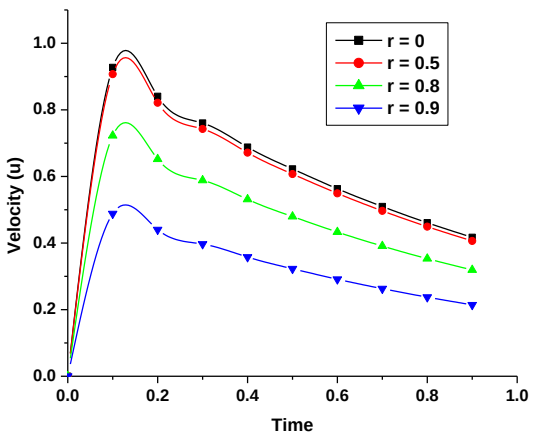

Fig. 7. Velocity profile for the air flow with time for different radial positions at Darcy number 10^{-1}

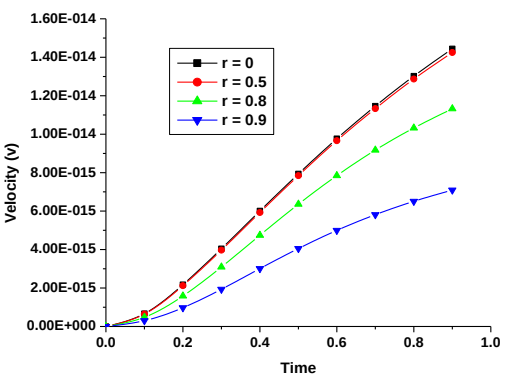

Fig. 8. Velocity profile for the particle with time for different radial positions at Darcy number 10^{-1}

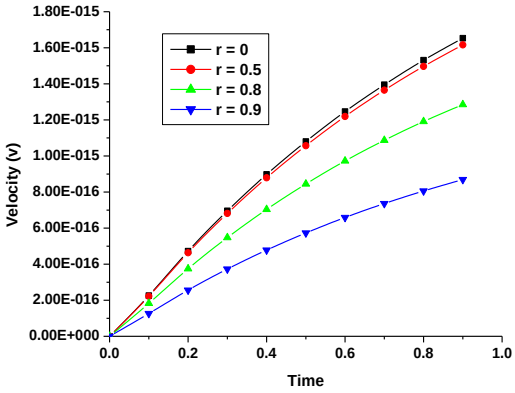

Fig. 9. Velocity profile for the particle with time for different radial positions at Darcy number 10^{-2}

5.4 Biofilter removal efficiency model

The removal efficiency is the most essential factor for the acting of a biofilter. Hodge and Devinny[10] developed the model for an idealized biofilter. The removal efficiency (R.E.) equation is written in dimensionless form as:

$$R.E. = 1 - \exp[-b_1 k_m t] \tag{15}$$

Where $_1$ is the biological degradation constant [time-1], k_m is the partitioning coefficient [dimensionless], and t is the traveling time of air flowing all the way through the biofilter [time]. The product of b_1 and k_m was selected for comparison to exhibit the effect of flow heterogeneity on biofilter removal. The product of the constants was selected so that the removal efficiency was 90% at $\varepsilon = 0.6$, and $Da = 10^{-3}$, where flow all the way through the biofilter was homogeneous. The time of travel of each particle was placed into Eq. (15) and the resultant removal efficiencies were averaged. The average removal efficiency of the particles was taken as the total biofilter removal efficiency for that simulation. A more complete derivation of the R.E. model can be established in [3, 4].

One of the purposes of this work is to get the best design of biofilter. Numerous studies were passed out to get better the removal efficiency with different methods[13, 15, 20]. One valuable way to get better removal efficiency is to formulate the traveling time of every one particle being identical. If we could plan a porous media with heterogeneous Darcy number and porosity values, then we could optimize the biofilter. In the current study, we have considered the average Darcy number of the entire porous media as constant.

Fig. 9 represents the entire removal efficiencies with average travel time for different values of Darcy number. It is exposed that for higher Darcy number, the removal efficiency increases extensively with decreasing Darcy number; on the other hand at lower Darcy number, i.e., $Da < 10^{-2}$ the increasing of the removal efficiency is simply decreasing Darcy number. The high removal efficiency will charge a large amount of traveling time, and shorter traveling time will be at the cost of high removal efficiency. Accordingly, we can prefer a suitable Darcy number to find preferred removal time or removal efficiency along with the definite requirements of the biofilter. The size of the pores and the particles conceptualize the design of biofilter in this study as per our observations.

6 Conclusion

The porous flow through biofilter medium (alveolar sacs) is numerically calculated by the finite difference method. The simulation outcomes direct to the following conclusions:
(1) The Darcy number has a leading persuade on the air velocity, as well as the particle velocity for the removal efficiency of the biofilter.

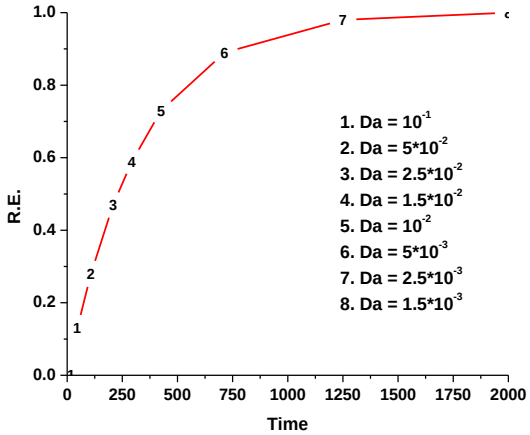

Fig. 10. Overall removal efficiencies with average traveling time for different Darcy numbers

(2) The Darcy number has also leading persuade on the air traveling time, as well as the removal efficiency of the biofilter.
(3) At low Darcy number, the effect of porosity on removal efficiency is very small. At high Darcy number, porosity considerably influences the removal efficiency, and porosity should be measured as a free parameter in this illustration.

References

[1] B. Anet, M. Lemasle, et al. Characterization of gaseous odorous emissions from a rendering plant by gc/ms and treatment by biofiltration. *Jounral of Environmental Management*, 2013, **128**: 981–987.
[2] Y. Cengel, J. Cimbala. Solutions manual for fluid mechanics: Fundamentals and applications. *McGraw-Hill Companies, Incorporation*, 2006.
[3] D. Chitwood. Two-stage biofilter for treatment of POTW off gases. *Civil Environmental Engineering*, 1999, **181**.
[4] D. Chitwood, J. Devinny, E. Meiburg. A computational model for heterogeneous flow through low headloss biofilter media. *Environmental Progress*, 2002, **21**(1): 11–19.
[5] H. Darcy. Les fontaines publiques de la ville de Dijon. *Dijon, Vector Dalmont, Paris*, 1856.
[6] N. Cameron, M. Mitchell. Nanoscale: Issues and perspectives for the nano century. *John Wiley, Hoboken, New Jersey*, 2007, **462**.
[7] F. Dullen. *Porous Media: Fluid Transport and Pore Structure*. *Academic press*, 1991.
[8] S. Ergun. Fluid flow through packed columns. *Chemical Engineering Process*, 1952, **48**: 89–94.
[9] J. Flora, R. Hargis, et al. The role of pressure drop and flow redistribution on modeling mercury control using sorbent injection in baghouse filters. *Journal of the Air & Waste Management Assocation*, 2006, **56**(3): 343–349.
[10] D. Hodge, J. Devinny. Modeling removal of air contaminants by biofiltration. *Jounral of Environmental Management*, 1995, **121**(1): 21–44.
[11] P. Hoet, I. Hohlfeld, O. Salata. Nanoparticles-known and unknown health risks. *Journal of Nanobiotechnology*, 2004, **2**(1): 12.
[12] H. Husain, B. P. Herner. Biofilter media to remove odour causing compounds from waste gas streams. *Biorem Technologies Incorporation*, 2014.
[13] H. Jang, M. Hirai, M. Shoda. Enhancement of styrene removal efficiency in biofilter by mixed cultures of pseudomonas sp sr-5. *Journal of bioscience and bioengineering*, 2006, **102**(1): 53–59.
[14] G. Kafle, L. Chen, et al. Field evaluation of wood bark-based down-flow biofilters for mitigation of odor, ammonia, and hydrogen sulfide emissions from confined swine nursery barns. *Journal of environmental management*, 2015, **147**: 164–174.
[15] Y. Ma, B. Yang, J. Zhao. Removal of h2s by thiobacillus denitrificans immobilized on different matrices. *Bioresource technology*, 2006, **97**(16): 2041–2046.
[16] L. Malhautier, S. Cariou, et al. Treatment of complex gaseous emissions emitted by a rendering facility using a semi-industrial biofilter. *Journal of Chemical Technology and Biotechnology*, 2014, **11**(21).

[17] M. Mayerhofer, J. Govaerts, et al. Experimental investigation of pressure drop in packed beds of irregular shaped wood particles. *Powder Technology*, 2011, **205**(1): 30–35.
[18] A. Nel, T. Xia, et al. Toxic potential of materials at the nanolevel. *Science*, 2006, **311**(5761): 622–627.
[19] P. Nithiarasu, K. Ravindran. A new semi-implicit time stepping procedure for buoyancy driven flow in a fluid saturated porous medium. *Computer methods in applied mechanics and engineering*, 1998, **165**(1): 147–154.
[20] M. Qasim, Z. Shareefdeen. Analysis of a recent biofilter model for toluene biodegradation. *Advances in Chemical Engineering and Science*, 2013, **3**: 57.
[21] J. Rizzolo, V. Santos, et al. Biofiltration of volatile organic compounds of Brazilian gasoline. *Brazilian Archives of Biology and Technology*, 2014, **57**(1): 119–125.
[22] P. Sharma. Free convection effects on the low past a porous medium bounded by a vertical infinite surface with constant saction and constant heat flux. *Journal of physics d-applied physics*, 1992, **25**: 162–166.
[23] G. Smith. *Numerical Solution of Partial Differential Equations*, Oxford University Press, 1985.
[24] K. Vafai. Convection flow and heat transfer in variable porous media. *Journal of Fluid Mechanics*, 1984, **147**: 233–259.
[25] Z. Wei, X. Liu, et al. Gas dimethyl sulfide removal in biotrickling filtration. Open Access Science Reports, 2013.
[26] W. Yan, Y. Liu, et al. Lattice boltzmann simulation on natural convection heat transfer in a two-dimensional cavity filled with heterogeneously porous medium. *International Journal of Modern Physics C*, 2006, **17**(06): 771–783.
[27] L. Zhao, S. Huangab, Z. Weia. A demonstration of biofiltration for voc removal in petrochemical industries. *Environmental Science: Processes & Impacts*, 2014, **16**(5): 1001–1007.